NACA

RESEARCH MEMORANDUM

A SIMULATOR STUDY OF SOME LONGITUDINAL STABILITY AND CONTROL PROBLEMS OF A PILOTED AIRCRAFT IN FLIGHTS

TO EXTREME ALTITUDE AND HIGH SPEED

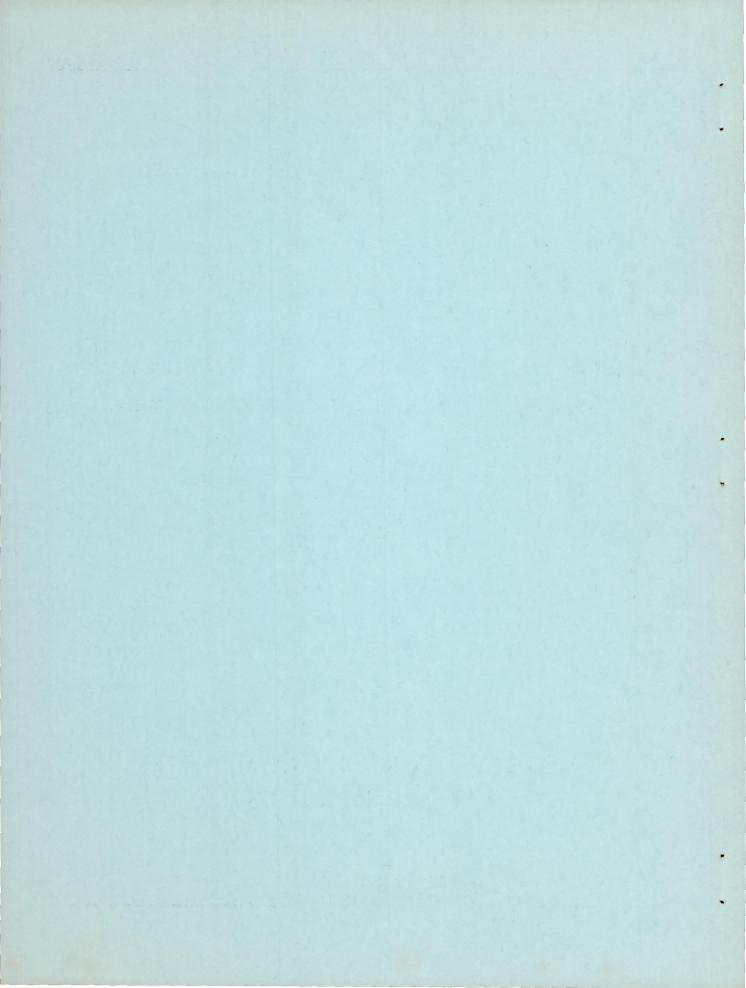
By Howard F. Matthews and Robert B. Merrick

Ames Aeronautical Laboratory Moffett Field, Calif.

NATIONAL ADVISORY COMMITTEE FOR AERONAUTICS

WASHINGTON

September 7, 1956 Declassified July 11, 1961



NATIONAL ADVISORY COMMITTEE FOR AERONAUTICS

RESEARCH MEMORANDUM

A SIMULATOR STUDY OF SOME LONGITUDINAL STABILITY AND

CONTROL PROBLEMS OF A PILOTED AIRCRAFT IN FLIGHTS

TO EXTREME ALTITUDE AND HIGH SPEED

By Howard F. Matthews and Robert B. Merrick

SUMMARY

A brief study utilizing pilots to "fly" a simulator has been made of some longitudinal stability and control problems of an assumed aircraft capable of flights to altitudes essentially out of the atmosphere. The results show that more than the inherent longitudinal damping of the aircraft is necessary to effect a safe flight, particularly during entry into the atmosphere. With a favored amount of additional damping, large changes in control sensitivity and period are acceptable. With this amount of damping provided, no strong preference was expressed for monitoring any particular quantity (attitude, angle of attack, or combinations thereof with normal acceleration) during the entry. Some data applicable to instrumentation and flight programming show that the peak altitude is considerably more sensitive to constant errors in angle of attack than in attitude during ascent.

INTRODUCTION

In recent years the development of high thrust, liquid-fuel, rocket engines has progressed so that a new phase of flight of a manned vehicle appears possible - that of flight essentially out of the atmosphere to several hundred thousands of feet and to Mach numbers near 6.

Besides problems in the fields of human behavior, heat dissipation, etc., such a flight poses stability and control problems associated with high altitude and high Mach number. One such problem is whether longitudinal-stability augmentation in the form of additional damping must be added to insure a safe ascent and entry into the atmosphere. This question provided the primary impetus for a brief simulator investigation of the longitudinal stability and control of an assumed high performance aircraft in flights to extreme altitudes. In addition to determining the

importance of increased damping, the effect of changes in period, control sensitivity, and piloting technique was also examined. The simulation was conducted in real time using three NACA Ames engineering test pilots, whose aggregate experience in flight test work was 18 years, to fly a simulator by instruments to a preselected flight plan. Thus the results are based, in part, on pilot opinion.

NOTATION

c_D	drag coefficient, $\frac{drag}{qS}$
$\mathtt{c}_\mathtt{L}$	lift coefficient, $\frac{\text{lift}}{\text{qS}}$
$c_{L_{\alpha}}$	lift-curve slope of complete airplane, $\frac{\partial C_L}{\partial \alpha}$
C_{m}	pitching-moment coefficient, $\frac{\text{pitching moment}}{\text{qS}\tilde{c}}$
c_{mit}	stabilizer-effectiveness parameter, $\frac{\partial C_m}{\partial i_t}$
$c_{m_{\alpha}}$	static-stability parameter, $\frac{\partial C_m}{\partial \alpha}$
$\frac{C_{m_{\bullet}\bar{c}} + C_{m_{\bullet}\bar{c}}}{2V} = \frac{\alpha \bar{c}}{2V}$	damping parameter, $\frac{\partial c_m}{\partial (\dot{\theta}\bar{c}/2V)} + \frac{\partial c_m}{\partial (\dot{\alpha}\bar{c}/2V)}$
D	differential operator, $\frac{\partial}{\partial t}$
IY	pitch moment of inertia, slug ft ²
K	gearing or gain
M	Mach number
R	radius of earth, 21.12×10 ⁶ ft
S	reference wing area, ft ²

```
velocity, ft/sec
          wing span, ft
            wing section chord, ft
C
             wing mean aerodynamic chord, \frac{\int_0^{b/2} c^2 dy}{\int_0^{b/2} c dy}, ft
ē
             gravitational acceleration, 32.2 ft/sec2
g
h
             altitude, ft
             incidence of stabilizer
it
             mass, slugs
m
             normal acceleration factor, g
n_{Z}
             dynamic pressure, \frac{1}{2} \rho V^2, lb/sq ft
q
             time, sec
t
             lateral coordinate of wing section chord, ft
У
             angle of attack
α
             flight path angle
y
             angular deflection of control stick, positive stick back
δcs
             damping ratio
5
             pitch attitude angle, \alpha + \gamma
θ
             density of air, slugs/cu ft
P
             natural frequency
ω
```

Subscripts

a airplane

g pitch rate gyro

- o steady state
- p potentiometer
- s servo

All angles are in radians unless otherwise noted. A dot (') above a symbol represents the first derivative with respect to time.

THE SIMULATOR AND PERTINENT ASSUMPTIONS

Description of the Simulator

The simulator can be considered to be composed of three parts, which with the pilot, form a closed loop system. These parts are a panel of flight instruments for visual observation by the pilot; a pilot's control stick; and an analog computer to solve the necessary equations describing the pitching motion, position in space, and changing mass characteristics of the aircraft.

The instrument panel. Figure 1 is a photograph of the instrument panel and pilot's control stick. From left to right and top to bottom on the panel, the instruments are flight path, angle of attack, normal acceleration, Mach number, dynamic pressure, gyro horizon, rate of climb, and altitude. The gyro horizon was simulated by a standard 5-inch DuMont oscilloscope. On the face of the oscilloscope can be seen a broken horizontal line representing the airplane and a vertical scale calibrated to give the attitude in degrees. The intense light of the flash when the photograph was taken obliterated the horizontal line generated by the beam of the scope to represent the horizon.

The flight instruments were simulated by voltmeters upon which appropriate scales had been drawn. All scales of angular quantities were in degrees, altitude in thousands of feet, climb in thousands of feet per minute, and dynamic pressure in pounds per square foot.

The two switches in the upper right-hand corner of the instrument panel are for the pilot to operate at his discretion. The use of the upper switch (speed brake) is self-explanatory. The lower switch (space control) when "on" introduces a moment into the pitching-moment equation which is proportional to the pilot's control stick deflection and is independent of dynamic pressure. This moment simulates that of a jet type of control and is used to change the attitude of the aircraft at altitudes where the density of the air is negligible.

5

The pilot's control stick. The pilot's control stick was a Sperry Flight Controller, Type No. B-4, commonly known as a formation stick. Its characteristics were:

- (a) Maximum deflection: 25° rearward, approximately 16° forward
- (b) Restoring moment: 12-inch ounces per degree
- (c) Time to return from 25° : 0.5 seconds to $12-1/2^{\circ}$, 4.0 seconds to neutral

The ratio between the stabilizer incidence and the pilot's control stick deflection was -1.6 unless otherwise noted.

The analog computer. The analog computer was of a standard type employing d-c operational amplifiers, servo-driven multipliers, and Reeves rotating drums modified for use as one-variable-input-function generators. These generators had an accuracy of about 1/10 of 1 percent full scale and two were used to cover the density range from an altitude of 30,000 to 200,000 feet (the density of air above 200,000 feet was assumed to be zero).

The Equations of Motion

The three-degree-of-freedom longitudinal equations of motion about the wind axis used are

$$m\dot{V} = T \cos \alpha - \frac{1}{2} \rho V^2 SC_D - mg \sin \gamma$$
 (1)

$$mV\left(\dot{\gamma} - \frac{V\cos\gamma}{R+h}\right) = T\sin\alpha + \frac{1}{2}\rho V^2SC_L - mg\cos\gamma \tag{2}$$

$$I_{\mathbf{Y}} = \frac{1}{2} \rho V^{2} S_{\mathbf{c}} \left[C_{\mathbf{m}_{\alpha}} + C_{\mathbf{m}_{\mathbf{i}_{\mathbf{t}}}} + \left(C_{\mathbf{m}_{\mathbf{i}_{\mathbf{t}}}} + C_{\mathbf{m}_{\mathbf{i}_{\mathbf{c}}}} + C_{\mathbf{m}_{\mathbf{i}_{\mathbf{c}}}} \right) - \frac{T_{\mathbf{0}}}{63.8} - \frac{T}{12} + 40008_{\mathbf{cs}}^{\circ} \right]$$
(3)

with the density being obtained from a density-altitude relationship, initial conditions, and the solution of the equation

$$\dot{h} = V \sin \gamma$$
 (4)

The simultaneous solution of these equations gives the time history of the altitide, flight path, and pitching motion of the aircraft.

Several of the terms in equations (2) and (3) are not included normally but were retained herein because of the high performance of the assumed aircraft. These are:

(a) The term, $\frac{\text{mV}^2\cos\gamma}{\text{R}+\text{h}}$, in equation (2) which arises from the rotation of the wind axis with respect to a fixed earth axis system. For the maximum velocities and altitudes subsequently reached in this study the magnitude of this term was small, being about twice that of the omitted change in the gravitational effect with altitude.

- (b) The damping term, $-\frac{T\dot{\theta}}{63.8}$, in equation (3) which arises from expending fuel (see ref. 1). The value of the constant used is based on certain geometric and propulsion properties of the assumed aircraft.
- (c) The moment proportional to thrust, $-\frac{T}{12}$, in equation (3) to simulate a possible 1-inch thrust misalinement with the center of gravity.
- (d) A constant multiple of the control stick deflection, $+40008^{\circ}_{cs}$, in equation (3) to simulate the operation of a jet-reaction control (space control) for use at extreme altitudes. The magnitude of the constant was selected so that full rearward deflection of the pilot's control stick gave 2° per second squared angular acceleration of the aircraft after all fuel was expended.

Note also that the simplification of substituting

$$\begin{pmatrix}
C_{\underline{m}} & + & C_{\underline{m}} & \frac{\dot{\sigma}}{2V} \\
\frac{\dot{\sigma}}{2V} & \frac{\dot{\sigma}}{2V} & \frac{\dot{\sigma}}{2V}
\end{pmatrix}$$

for

$$\begin{array}{ccc} C_{m_{\stackrel{\bullet}{\mathcal{O}}\overline{c}}} & \frac{\mathring{\sigma}\overline{c}}{2V} + C_{m_{\stackrel{\bullet}{\mathcal{O}}\overline{c}}} & \frac{\mathring{\sigma}\overline{c}}{2V} \\ & & & & & \\ \end{array}$$

was made in equation (3) because of the limited capacity of the analog computer.

Assumptions

Atmospheric characteristics. The variation of temperature (for the computation of M) and density with altitude was taken from the tables of the International Civil Aviation Organization Standard Atmosphere (ref. 2) up to and including 20 kilometers (65,250 feet). For altitudes of 26 kilometers (85,306 feet) and above data from rocket soundings (ref. 3) were used. The characteristics between these two altitudes were obtained from a graphical fairing.

The aircraft and its characteristics. The triangular-wing model of reference 4 was used as being a representative aircraft for this study. A sketch of this aircraft and the assumed pertinent dimensional, mass, and propulsion characteristics are given in figure 2.

The lift and drag characteristics shown in figure 3 were obtained by fairing, interpolating, and extrapolating the data given in references 4, 5, and 6. Only the positive lift-coefficient data are shown, the negative being a mirror image about the $C_{\rm L}$ = 0 line. A $\triangle C_{\rm D}$ of 0.1, independent of Mach number, was added to simulate opening of the speed brakes.

The pitching-moment data of figure 4 were estimated, data below a Mach number of 2 not being included because of the limited capacity of the computer. For this reason, also, an average value of the speed of sound of 1,000 feet per second was used in computing the damping parameter.

Variables affecting pilot opinion. In general, the variables affecting pilot opinion are the control-force characteristics, pilot motion stimuli, and the dynamics of the aircraft. Because of the large magnitudes of longitudinal acceleration possible, it was surmized that a formation stick or similar control would be moved by wrist action from a restrained arm. Thus, it was anticipated that the stick-force characteristics would be of secondary importance, and therefore are unchanged with respect to the deflection of the stick throughout this investigation. Since this study was exploratory in nature and simplicity was important, physical motion of the pilot in pitch was not added to the simulation. From a relative importance viewpoint this omission as well as the invariance of the force characteristics are justified by the results of reference 7.

The remaining and most important variables are those of the dynamics of the aircraft as manifested through the monitored quantities. These variables are assumed to be the period, damping ratio, and control sensitivity $(V\dot{\gamma}/\delta_{\text{CS}})$ being used as a measure of this quantity) of the short-period mode of the augmented airplane. For subsequent correlation purposes formulas approximating these characteristics were developed in the usual manner by first linearizing the normal-force and pitching-moment equations to give in operator notation

$$\dot{\theta} - \left[D + \left(\frac{T \cos \alpha_{O}}{mV} + \frac{qS}{mV} C_{L_{CL}}\right)\right]\alpha = 0$$

$$\boxed{ D - \frac{qS\bar{c}}{I_Y} \left(C_{\underline{m}\underline{\dot{e}}\bar{c}} + C_{\underline{m}\underline{\dot{c}}\bar{c}} \right) \frac{\bar{c}}{2V} + \frac{T}{63.8I_Y}} \dot{\theta} - \frac{qS\bar{c}}{I_Y} C_{\underline{m}_C} \alpha = \frac{qS\bar{c}}{I_Y} C_{\underline{m}_{\dot{1}}\dot{c}} i_{\dot{1}} i_{\dot{1}}$$

where the angles are now perturbations about the steady state. The necessary aerodynamic transfer functions were found easily from the above equations to be

$$\frac{\dot{\theta}}{i_{t}} \stackrel{\cong}{=} \frac{-\frac{C_{m_{\dot{1}t}}}{C_{m_{\alpha}}} \left(\frac{T \cos \alpha_{o}}{mV} + \frac{qS}{mV} C_{L_{\alpha}}\right) \left(1 + \frac{D}{\frac{T \cos \alpha_{o}}{mV} + \frac{qS}{mV} C_{L_{\alpha}}}\right)}{\frac{T \cos \alpha_{o}}{mV} + \frac{qS}{mV} C_{L_{\alpha}} - \frac{qS\bar{c}}{I_{Y}} C_{m_{\dot{\alpha}}\bar{c}} + C_{m_{\dot{\alpha}}\bar{c}} \frac{\bar{c}}{2V} + \frac{T}{63.8I_{Y}}}{\frac{QS\bar{c}}{I_{Y}} C_{m_{\alpha}}}$$

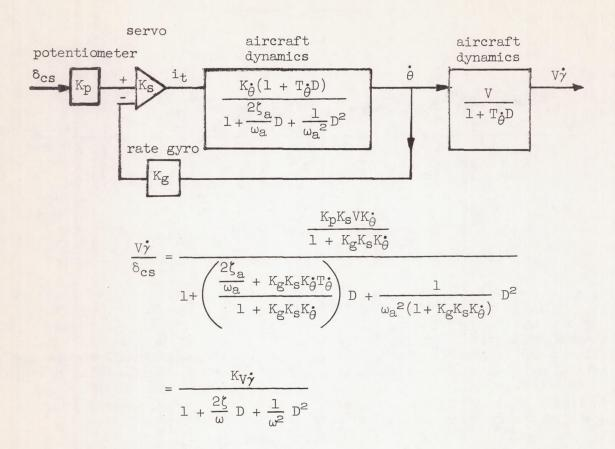
$$-\frac{qS\bar{c}}{I_{Y}} C_{m_{\alpha}}$$

$$D + \frac{D^{2}}{-\frac{qS\bar{c}}{I_{Y}} C_{m_{\alpha}}}$$

and

$$\frac{\frac{V\dot{\gamma}}{\dot{\theta}}}{\dot{\theta}} = \frac{V}{1 + \frac{D}{\frac{T \cos \alpha_{O}}{mV} + \frac{qS}{mV} C_{L_{\alpha}}}}$$

The well-known techniques of servomechanism theory were then applied to obtain the characteristics of the airplane-autopilot combination. An illustrative block diagram of the simplified augmented control system assumed herein and the resulting dynamic characteristic formulas follow:



or control sensitivity,

$$K_{\mbox{W}\mbox{$\stackrel{\bullet}{\gamma}$}} = \frac{-\left(\mbox{$K_{\mbox{g}}$}\mbox{$K_{\mbox{W}\mbox{κ}}$}\right) \left(\frac{\mbox{$\frac{T}{m}$}}{\mbox{cos}} \mbox{cos} \mbox{$\alpha_{\mbox{$o$}}$} + \frac{\mbox{$\frac{qS}{m}$}}{\mbox{c}} \mbox{$C_{\mbox{$L_{\mbox{α}}$}}\right) \frac{\mbox{$C_{\mbox{$m_{\mbox{$\omega$}}$}}}}{\mbox{$C_{\mbox{$m_{\mbox{ω}}$}}$}} \\ = \frac{-\left(\mbox{$K_{\mbox{$g$}}$}\mbox{$K_{\mbox{$g$}}$}\right) \left(\frac{\mbox{T}}{\mbox{m}} \mbox{cos} \mbox{$\alpha_{\mbox{$o$}}$} + \frac{\mbox{qS}}{\mbox{m}} \mbox{$C_{\mbox{$L_{\mbox{α}}$}}\right) \frac{\mbox{$C_{\mbox{$m_{\mbox{$\omega$}}$}}}}{\mbox{$C_{\mbox{$m_{\mbox{ω}}$}}$}} \\ = \frac{-\left(\mbox{$K_{\mbox{$g$}}$}\mbox{$K_{\mbox{$g$}}$}\right) \left(\frac{\mbox{T}}{\mbox{m}} \mbox{cos} \mbox{$\alpha_{\mbox{$o$}}$} + \frac{\mbox{qS}}{\mbox{m}} \mbox{$C_{\mbox{$L_{\mbox{ω}}$}}$}\right) \frac{\mbox{$C_{\mbox{$m_{\mbox{ω}}$}}}}{\mbox{$C_{\mbox{$m_{\mbox{$\omega$}}$}}}} \\ = \frac{-\left(\mbox{$K_{\mbox{$g$}}$}\mbox{$K_{\mbox{$\omega$}}$}\right) \left(\frac{\mbox{T}}{\mbox{m}} \mbox{cos} \mbox{$\alpha_{\mbox{$o$}}$} + \frac{\mbox{qS}}{\mbox{m}} \mbox{$C_{\mbox{$L_{\mbox{ω}}$}}$}\right) \frac{\mbox{$C_{\mbox{$m_{\mbox{ω}}$}}}}{\mbox{$C_{\mbox{$m_{\mbox{$\omega$}}$}}$}} \\ = \frac{-\left(\mbox{$K_{\mbox{$g$}}$}\mbox{$K_{\mbox{$M_{\mbox{ω}}$}}\mbox{$M_{\mbox{ω}}$}} + \frac{\mbox{$q$}}{\mbox{$m_{\mbox{ω}}$}} \mbox{$C_{\mbox{ω}}$}} \right) \frac{\mbox{$C_{\mbox{$m_{\mbox{$\omega$}}$}}}}{\mbox{$C_{\mbox{$m_{\mbox{ω}}$}}}} \\ = \frac{-\left(\mbox{$K_{\mbox{$g$}}$}\mbox{$K_{\mbox{$M_{\mbox{ω}}$}}\mbox{$M_{\mbox{ω}}$} + \frac{\mbox{$q$}}{\mbox{$m_{\mbox{ω}}$}} \mbox{$C_{\mbox{ω}}$} \right) \frac{\mbox{$C_{\mbox{ω}}$}}{\mbox{$C_{\mbox{ω}}$}} \\ = \frac{-\left(\mbox{$K_{\mbox{$g$}}$}\mbox{$K_{\mbox{$\omega$}}$}\mbox{$M_{\mbox{$\omega$}}$}} + \frac{\mbox{q}}{\mbox{$M_{\mbox{$\omega$}}$}} \mbox{$C_{\mbox{$\omega$}}$} \mbox{$M_{\mbox{$\omega$}}$} \mbox{$C_{\mbox{$\omega$}}$} \right) \frac{\mbox{$C_{\mbox{$\omega$}}$}}{\mbox{$M_{\mbox{$\omega$}}$}} \\ = \frac{-\left(\mbox{$K_{\mbox{$\omega$}}$}\mbox{$K_{\mbox{$\omega$}}$}\mbox{$M_{\mbox{$\omega$}}$}} \mbox{$M_{\mbox{$\omega$}}$} \mbox{$M_{\mbox{$\omega$}}$} \mbox{$M_{\mbox{$\omega$}}$} \mbox{$M_{\mbox{$\omega$}}$} \mbox{$M_{\mbox{$\omega$}}$} \mbox{$M_{\mbox{$\omega$}}$} \mbox{$$

undamped short period,

$$\frac{2\pi}{\omega} = \frac{2\pi}{\left(-\frac{qS\bar{c}}{I_{Y}} C_{m_{\alpha}}\right) \left[1 - (K_{g}K_{s})\left(\frac{T}{mV} \cos \alpha_{o} + \frac{qS}{mV} C_{L_{\alpha}}\right) \frac{C_{m_{i_{t_{t}}}}}{C_{m_{\alpha}}}\right]^{1/2}}$$

damping ratio,

$$\zeta = \frac{\frac{T}{mV} \cos \alpha_{o} + \frac{qS}{mV} C_{L_{\alpha}} - \frac{qS\bar{c}}{I_{Y}} \left(C_{m} \frac{\dot{\theta}\bar{c}}{2V} + C_{m} \frac{\dot{\alpha}\bar{c}}{2V} \right) \frac{\bar{c}}{2V} + \frac{T}{63.8I_{Y}} + (K_{g}K_{s}) \frac{qS\bar{c}}{I_{Y}} C_{m_{i_{t}}}$$

$$\left\{ \left(-\frac{qS\bar{c}}{I_{Y}} C_{m_{\alpha}} \right) \left[1 - (K_{g}K_{s}) \left(\frac{T}{mV} \cos \alpha_{o} + \frac{qS}{mV} C_{L_{\alpha}} \right) \frac{C_{m_{i_{t}}}}{C_{m_{\alpha}}} \right] \right\}^{1/2}$$

RESULTS AND DISCUSSION

Preliminary Considerations

Prior to the pilots'flying the simulator, a number of programmed exploratory flights were made for the purpose of selecting some few as standards for pilot-opinion evaluation. An example of such a flight is illustrated in figure 5 for which it was assumed that the aircraft was initially released from a "mother" airplane at M=0.6 and an altitude of 35,000 feet, with angle of attack being programmed in the manner shown. In figure 5(b) are plotted the three parameters which are assumed to characterize the dynamics of the aircraft and to influence pilot opinion.

From a control aspect such a flight may be divided roughly into ascent to the upper atmosphere (defined herein as 200,000 feet and above), the ballistic trajectory in the upper atmosphere, and the entry into the denser lower atmosphere and establishment of level flight. Since the problems associated with each of these divisions were not of the same magnitude and the simulator had to be run at true time, it was expedient to investigate them separately. These preliminary runs also indicated that entry was the most difficult to control, probably due to the more rapid change in the dynamic characteristics; therefore this phase of the flight was examined in considerably more detail than the others.

Certain results of the survey of programmed entry flights are summarized in table I. These results were obtained by beginning the entry at an altitude of 200,000 feet with appropriate initial conditions from zenith. Shown in figures 6, 7, and 8 are representative time histories of the three types of programmed flights noted in the table. Of particular interest is that the constant attitude entry, which has automatic control advantages, inherently programs the angle of attack in such a manner as to result in relatively low accelerations.

The programmed entry of figure 6 was selected as an initial reasonable standard for the pilot to match. The speed-brakes-off condition was chosen,

NACA RM A56F07

since, besides simulating the possible failure of the brakes, it also approximately represents conditions wherein a descent is made from a considerably higher altitude at higher accelerations with speed brakes on.

Entry

Effect of increased damping.— A representative "piloted" standard entry flight without artificial damping is shown in figure 9(a). For this and all other flights the pilot was required to correct an initial error. In general, all three pilots developed sufficient proficiency by practice to effect an entry comparable to that shown in the figure if, as shown by the it record, no effort were made to damp out any oscillations. However, as illustrated in figure 9(b), any attempt to reduce the magnitude of the motions of the aircraft by corrective movements of the stabilizer by the pilot frequently led to intensifying the oscillations to destructive magnitudes. For this reason the pilots were unanimous in their opinion that additional damping by artificial means was necessary.

Plotted in figure 10 are the dynamic characteristics of the aircraft for the standard entry flight with and without artificial damping. Figures 11(a), (b), and (c) are time histories of representative piloted flights for each of the feedback gearings noted in figure 10. These results show progressively less difficulty in controlling the angle of attack and normal acceleration as the damping is increased. The pilots rated the lowest gearing acceptable but considered as desirable the damping provided by either of the two highest feedback gearings and a slight preference was shown for the 0.6 value.

It should be noted that the increased damping was obtained without the use of a gain changer and that the control motions necessary to provide the damping $(K_gK_s\dot{\theta})$ were only a maximum of 3.5°.

Effect of period and control sensitivity. Since the previous results indicated that additional damping was necessary, the effect of period and control sensitivity was determined by using the entry flight with a feedback gearing of -0.6 as a revised standard for comparison. Figure 12 shows the computed dynamic entry characteristics for the two extremes in period investigated as compared with the revised standard. The changes in the values of $C_{m_{\alpha}}$, $C_{m_{\dot{1}+}}$, and feedback gearing necessary to achieve the varia-

tion in period only are also noted in the figure. Representative time histories of piloted flights for the two changes in period are not given since they differ little in appearance from figure ll(b).

The pilots' conclusions on the effect of the change in period were not entirely in agreement. One expressed a mild preference for the longer period. Another considered the longer period as being too long and would

have chosen the shorter period if it had somewhat greater damping. In general, the pilots favored the combination of dynamic characteristics given in figure ll(b) and used here as the revised standard.

This revised standard entry flight also was made with a decrease in the sensitivity of the control from a i_t/δ_{cs} of -1.6 to -1.0. However, no marked preference was given by the pilots for the less sensitive control.

Pilot opinion correlation.— In figure 13 are shown partial results of a Cornell Aeronautical Laboratory pilot opinion flight evaluation of variations in the longitudinal short period dynamic characteristics using a variable-stability F-94 airplane (ref. 8). The dashed boundary lines, ratings, and pertinent pilots' objections were taken from the referenced report and are specified for a fighter-type aircraft. The rating of "unacceptable" refers to the aircraft's inability to accomplish its mission as a fighter and not necessarily that it is unsafe to fly.

Plotted as overlayed solid lines in figure 13 and identified by number or letter are the computed dynamic characteristics from figures 10 and 12 for the constant $n_{\rm Z}$ portion of the entry. The associated pilots' opinions have been given in previous paragraphs and briefly are that the lowest damping ratio was clearly unsatisfactory and that an average damping ratio of 0.6 and a frequency of 0.3 cycles per second was preferred over the other acceptable combinations tested. It is apparent that the Ames pilots' opinions would match those of reference 8 more closely but for the tendency of the Ames pilots to upgrade the lower frequencies. However, although a lower frequency may be unsatisfactory for a fighter aircraft, it may be satisfactory for the instrument flying required for the type of flights considered herein.

Comments on entry technique. During the course of this investigation some flights were made monitoring different quantities during the entry for a feedback gearing of -0.6 and the normal pitching-moment aerodynamics. These additional quantities were maintaining constant attitude to a specified normal acceleration and maintaining constant attitude all the way, the attitude being indicated by the moving line on the scope (gyro horizon) representing the horizon. In general, reference to attitude rather than angle of attack was preferred, although not strongly, with constant attitude all the way selected as best. The pilots' reasons for these choices were that attitude gave a quicker indication of the airplane's dynamic motion than angle of attack; and that with attitude alone they were relieved of making at the proper time the transition from monitoring the gyro horizon or the angle-of-attack indicator to monitoring the normal accelerometer.

Additional flights also were made to assess the use of a gyro horizon wherein the line generated by the beam on the scope represents the airplane rather than the horizon. This type of presentation was favored by

NACA RM A56F07

a majority of the pilots, since the sense of movement of the line now corresponded to that of the angle-of-attack indicator and the normal accelerometer.

Control in Ascent and the Ballistics Trajectory

Thrust misalinement. Although the correction of entry control difficulties by means of increased damping would appear to eliminate dynamic problems during ascent, a few flights, nevertheless, were made to observe the effect of a 1-inch thrust misalinement. For this purpose an ascent programmed similar to that shown in figure 5 was used as a standard for the pilot to match. However, as noted previously, it was not possible to program on the computer the pitching-moment characteristics below a Mach number of 2. Thus, of necessity, the ascent was begun by the pilot at M = 2 and an altitude of 53,000 feet with the task of holding zero angle of attack.

In figure 14 are shown the results of such a piloted flight. From these data it is seen that the pilot could not prevent an appreciable pitch-up in angle of attack from occurring after burnout due to the long period and low control effectiveness. However, the low dynamic pressure at the altitude of burnout, which is the primary cause of the poor controllability, offsets the large change in angle of attack so that the effect on the acceleration is negligible. It is surmized that if burnout had occurred at a much lower altitude, a similar end result on acceleration would be obtained for the pilot would now have sufficient control to prevent a large change in angle of attack.

Peak altitude control. During the piloted flights of ascent a significant variation in the peak altitude reached was observed for repeated flights. These differences were traceable primarily to the inability of the pilot to maintain precisely zero angle of attack throughout the ascent. Since a higher peak altitude accentuates entry problems, it was of interest to determine the sensitivity of the maximum altitude to errors in the angle of attack or other monitored quantities. Plotted in figure 15 are some results obtained along this line for ascents similar to that shown in figure 5 wherein the data for attitude control were obtained by using the same initial conditions (M = 2, h = 53,000 ft) as for angle-of-attack control. It is seen from the figure that the peak altitude is about four times as sensitive to constant errors in the programmed angle of attack as to constant errors in attitude. This is of some importance in instrumentation and flight programming.

Control during ballistic trajectory. As noted previously, control during this portion of the flight (space control) is assumed to be by means of a small jet on a lever arm to provide a moment. The magnitude of the moment used herein was such as to result in 0.08° per second squared

angular acceleration for each degree of stick deflection or 2° per second squared maximum. Since there are neither damping nor restoring moments, some difficulty in control was anticipated but did not materialize. For example, figure 16 shows a representative flight in this region wherein the pilots' assignment was to maintain zero angle of attack to peak altitude and then change to 20° and hold for entry. As is evident from the flight simulator record, no difficulty was encountered in accomplishing this task for a single degree of freedom.

CONCLUSIONS

A brief investigation of some problems associated with the longitudinal control of an assumed high-speed aircraft in flights to altitudes essentially out of the atmosphere has been made by means of pilots "flying" a simulator. From the results of this study the following conclusions are drawn:

- l. Additional damping of the aircraft by artificial means must be provided to effect a safe flight, particularly during entry into the atmosphere. A favored amount of additional damping is that which will give about 0.6 critical damping near the entry pull-out altitude of 83,000 feet.
- 2. With a favored amount of additional damping, the pilots report large changes in period and control sensitivity are acceptable.
- 3. With additional damping provided, the pilots mildly favor monitoring constant attitude all the way during entry rather than maintaining constant attitude to a specified normal acceleration or maintaining constant angle of attack to a specified normal acceleration.
- 4. The constant attitude entry has advantages besides ease of automatic programming in that it inherently programs the angle of attack in such a manner as to result in relatively low longitudinal and normal accelerations.
- 5. The peak altitude reached is considerably more affected by constant errors in angle of attack than in attitude during ascent. This fact is of some importance in flight programming and instrumentation.
- 6. No difficulty is encountered in single-degree-of-freedom control during the ballistic portion of the trajectory.

Ames Aeronautical Laboratory
National Advisory Committee for Aeronautics
Moffett Field, Calif., June 7, 1956

REFERENCES

- 1. Barton, M. V.: The Effect of Variation of Mass on the Dynamic Stability of Jet-Propelled Missiles. Jour. Aero. Sci., vol. 17, no. 4, Apr. 1950, pp. 197-203.
- 2. International Civil Aviation Organization and Langley Aeronautical Laboratory: Manual of the ICAO Standard Atmosphere. Calculations by the NACA. NACA TN 3182, 1954.
- 3. The Rocket Panel: Pressures, Densities, and Temperatures in the Upper Atmosphere. The Physical Review, vol. 88, no. 5, Dec. 1952, pp. 1027-1032.
- 4. Neice, Stanford E., Wong, Thomas J., and Hermach, Charles A.: Lift, Drag, and Static Longitudinal Stability Characteristics of Four Airplane-Like Configurations at Mach Numbers From 3.00 to 6.28.

 NACA RM A55C24, 1955.
- 5. Hall, Charles F.: Lift, Drag, and Pitching Moment of Low-Aspect-Ratio Wings at Subsonic and Supersonic Speeds. NACA RM A53A30, 1953.
- 6. Reller, John O., Jr., and Hamaker, Frank M.: An Experimental Investigation of the Base Pressure Characteristics of Nonlifting Bodies of Revolution at Mach Numbers From 2.73 to 4.98. NACA TN 3393. 1955.
- 7. Investigation of Control "Feel" Effects on the Dynamics of a Piloted Aircraft System. BuAer Rep. No. AE-61-10, 25 Apr. 1955.
- 8. Harper, Robert P., Jr.: Flight Evaluations of Various Longitudinal Handling Qualities in a Variable-Stability Jet Fighter. WADC TR 55-299, July 1955.

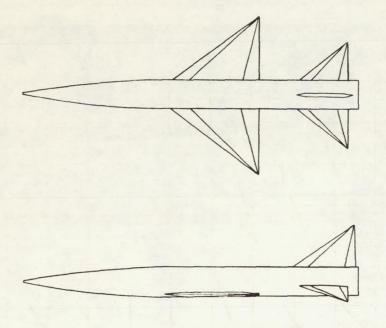
TABLE I. - RESUME OF PROGRAMMED ENTRY RESULTS

Descent from peak altitude of	Type entry	Speed brakes on				Speed brakes off			
		qmax lb/sq ft	M (max. q)	(Vý/g) _{max}	(-v/g) _{max}	qmax lb/sq ft	M (max. q)	(Vý/g) _{max}	(-V/g) _{max}
260,000 feet	$\alpha = 15^{\circ} \text{ to } n_{z} = 3.0$	1120	4.7	1.8	2.6	2400	5.6	2.0	1.2
	3.5	1020	4.8	2.3	2.6	1700	5.6	2.4	1.2
	4.0	950	4.9	2.6	2.6	1430	5.6	2.8	1.2
	4.5	880	5.0	3.1	2.6	1270	5.6	3.4	1.4
	5.0	820	5.1	3.5	2.7	1120	5.6	3.8	1.5
	$\alpha = 20^{\circ}$ to $n_z = 3.0$	830	4.8	1.7	2.2	1310	5.6	2.0	.9
	3.5	710	4.9	2.1	2.1	1010	5.6	2.4	1.0
	4.0	630	4.9	2.6	2.1	800	5.5	2.8	1.2
	4.5	570	5.1	3.0	2.2	720	5.5	3.3	1.4
	5.0	550	5.1	3.4	2.4	660	5.4	3.7	1.6
	$\alpha = 25^{\circ} \text{ to } n_z = 3.0$	670	4.7	1.6	1.9	960	5.4	2.0	.9
	3.5	560	4.8	2.0	2.0	690	5.3	2.3	1.1
	4.0	480	4.8	2.4	2.0	610	5.3	2.7	1.2
	4.5	430	4.8	2.8	2.1	520	5.2	3.1	1.4
	5.0	410	4.8	3.2	2.3	470	5.2	3.4	1.6
	Constant $\alpha = 15^{\circ}$	810	5.0	4.4ª	3.1ª	1040	5.4	5.5ª	2.3ª
	Constant $\alpha = 20^{\circ}$	560	5.0	4.48	2.9 ⁸	650	5.4	5.2ª	2.3ª
	Constant $\alpha = 25^{\circ}$	400	5.0	4.2ª	2.8ª	440	5.2	4.7ª	2.4ª
	$b_{Constant \theta} = 0^{\circ}$	750	4.6	2.3ª	1.8ª	1200	5.4	2.4ª	1.0ª
	Constant $\theta = 5^{\circ}$	510	4.8	2.3ª	1.7ª	700	5.2	2.5ª	1.1ª
344,000 feet	$\alpha = 15^{\circ} \text{ to } n_{z} = 4.0$	1750	4.1	2.6	3.8				
	4.5	1550	4.2	3.1	3.6				
	5.0	1360	4.2	3.5	3.5	2900	5.1	3.8	1.6
	$\alpha = 20^{\circ} \text{ to } n_{Z} = 4.0$	1320	4.2	2.6	3.2		-	3.0	
	4.5	1180	4.3	3.1	3.1	2200	5.0	3.3	1.4
	5.0	1040	4.4	3.4	3.0	1800	5.2	3.7	1.4
	$\alpha = 25^{\circ} \text{ to } n_z = 4.0$	1120	4.2	2.6	2.9	2100	5.1	2.8	1.3
	4.5	970	4.5	3.0	2.7	1520	5.1	3.3	1.3
	5.0	880	4.5	3.4	2.8	1200	5.2	3.7	1.3
	Constant $\alpha = 15^{\circ}$	1150	4.8	6.5ª	4.2ª			-	
	Constant $\alpha = 20^{\circ}$	780	4.6	6.7ª	4.0a				
	Constant $\alpha = 25^{\circ}$	560	4.6	6.5ª	3.9ª	640	4.9	7.4a	3.4a
	bConstant $\theta = -2^{\circ}$	780	4.2	3.5ª	2.2ª	≈1200	5.0	3.6ª	1.4ª

 $^{\rm a}_{\rm Does}$ not occur at maximum $\,$ q; all others do closely. $^{\rm b}_{\rm Will}$ not recover to level flight; entry ends in mild dive.



Figure 1.- Pilot control stick and instrument panel.



Dimensional:

 $S = 200 \text{ ft}^2$ $\bar{c} = 10.9 \text{ ft}$ $i_{t_{max}} = -40^\circ, +25^\circ$

Mass:

W = 30,000 lb gross, 12,000 burnout $I_Y = 75,000 \text{ slug-feet}^2 \text{ gross}, 50,000 \text{ burnout}$

Propulsion:

T = 60,000 lb; Specific impulse = 260 sec; Propulsion time = 78 sec

Figure 2.- The assumed aircraft and certain pertinent characteristics.

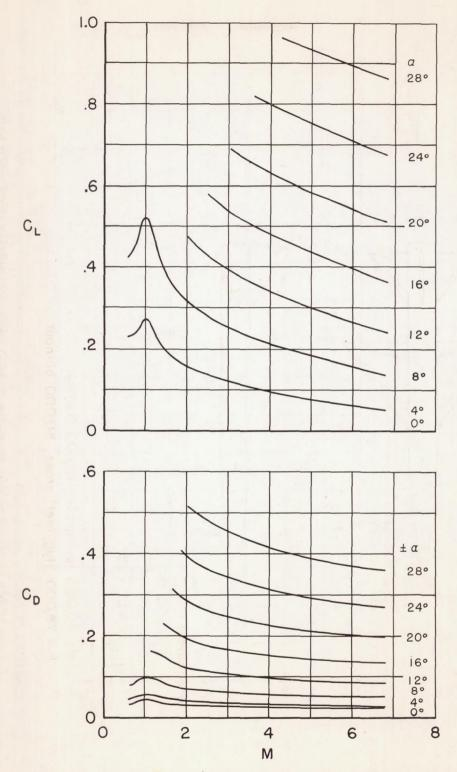
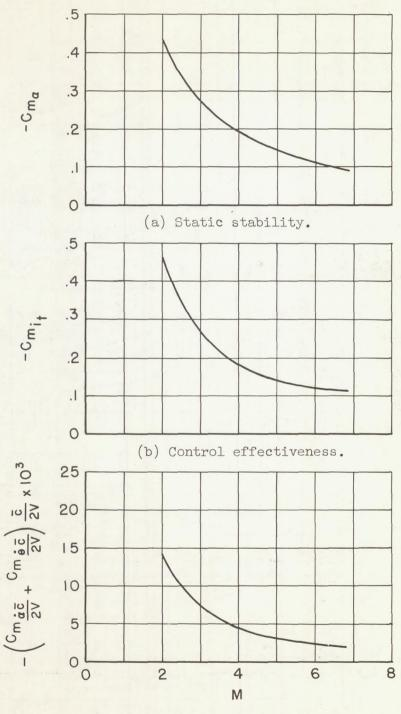
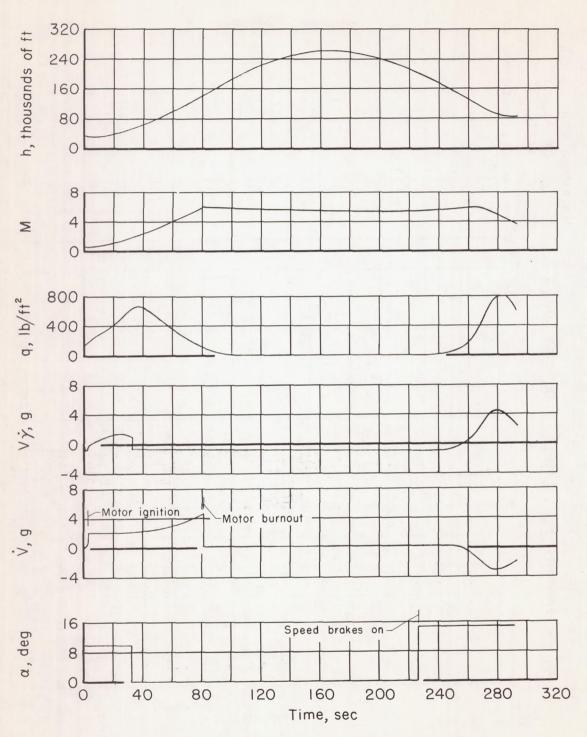


Figure 3.- Assumed lift and drag characteristics.



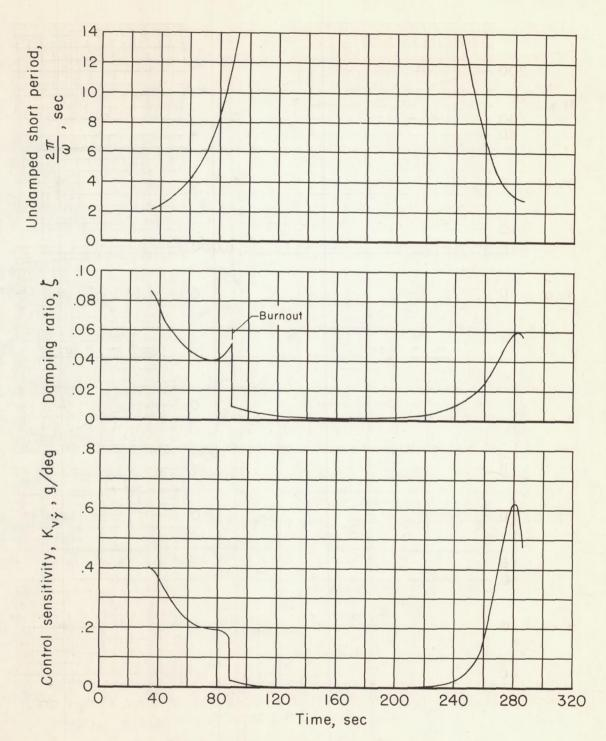
(c) Damping parameter.

Figure 4.- Assumed aerodynamic pitching-moment characteristics.



(a) Steady-state conditions.

Figure 5.- Flight to an altitude of 260,000 feet and return; programmed angle of attack.



(b) Computed dynamic characteristics.

Figure 5.- Concluded.

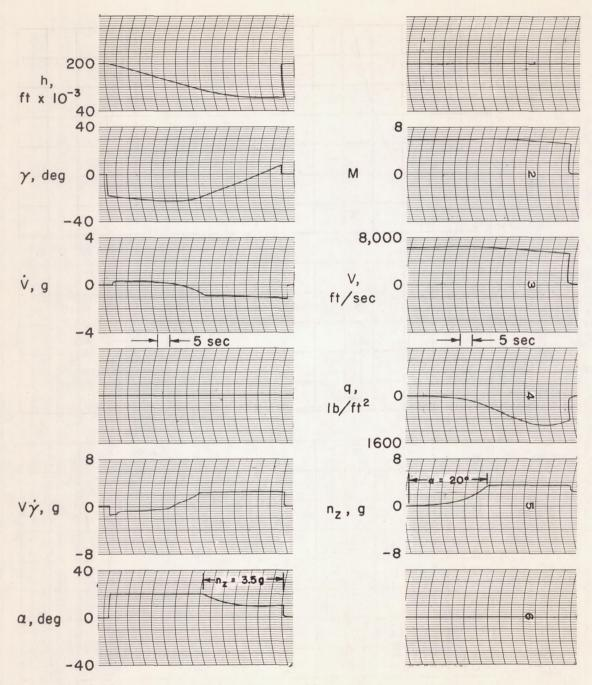


Figure 6.- Entry from 260,000-foot peak altitude; speed brakes off, programmed α = 200 to n_z = 3.5g.

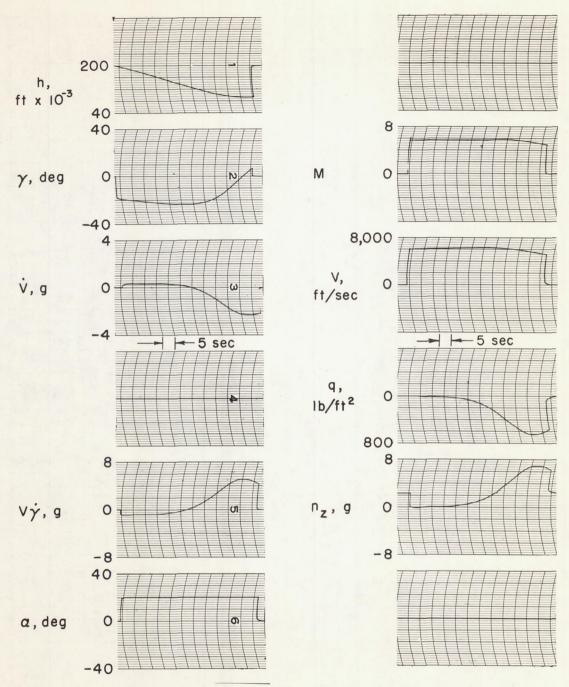


Figure 7.- Entry from 260,000-foot peak altitude; speed brakes off, programmed $\alpha = 20^{\circ}$.

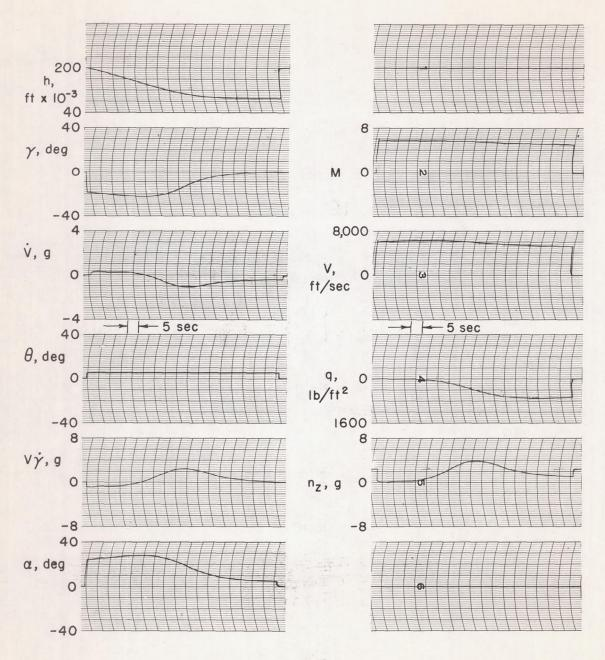
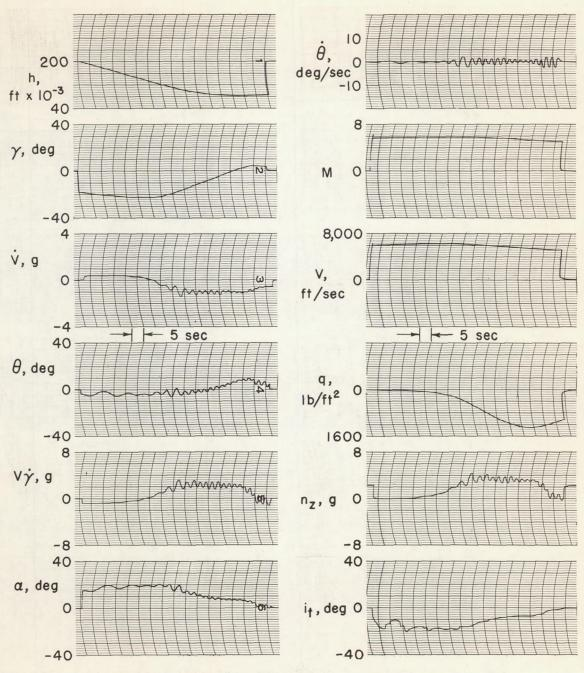
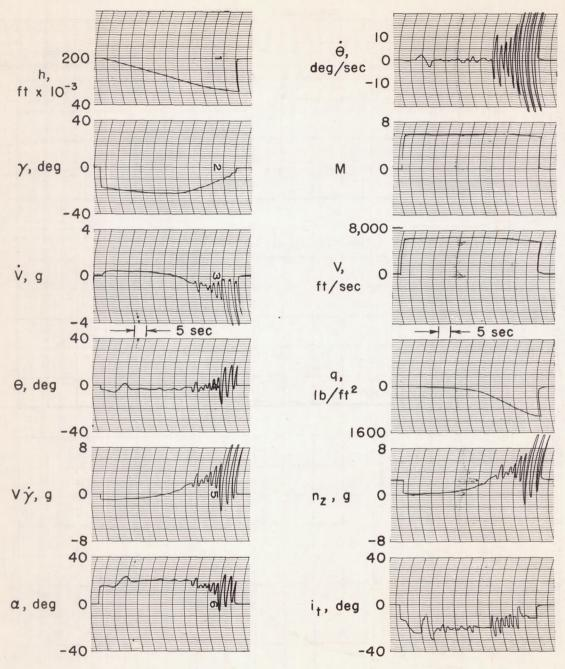


Figure 8.- Entry from 260,000-foot peak altitude; speed brakes off, programmed $\theta = 5^{\circ}$.



(a) No attempt by pilot to damp oscillations.

Figure 9.- Standard piloted entry flight; no artificial damping.



(b) Damping of oscillations attempted by pilot.

Figure 9.- Concluded.

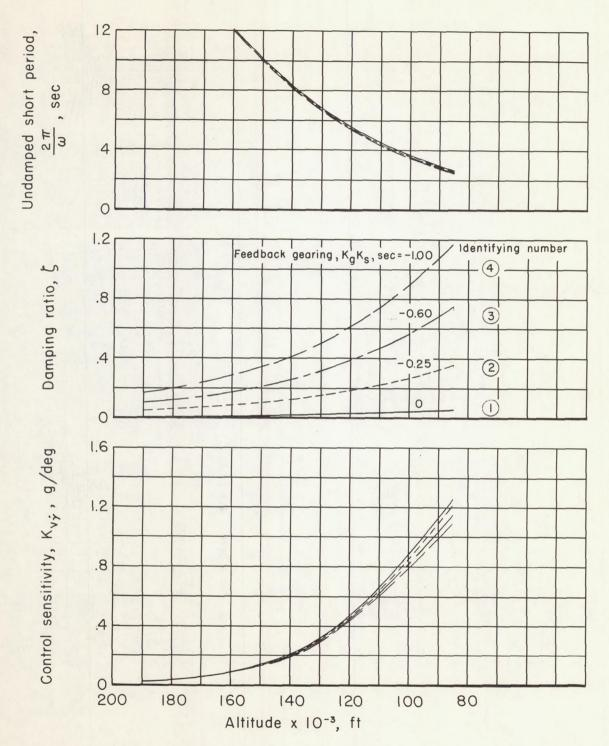
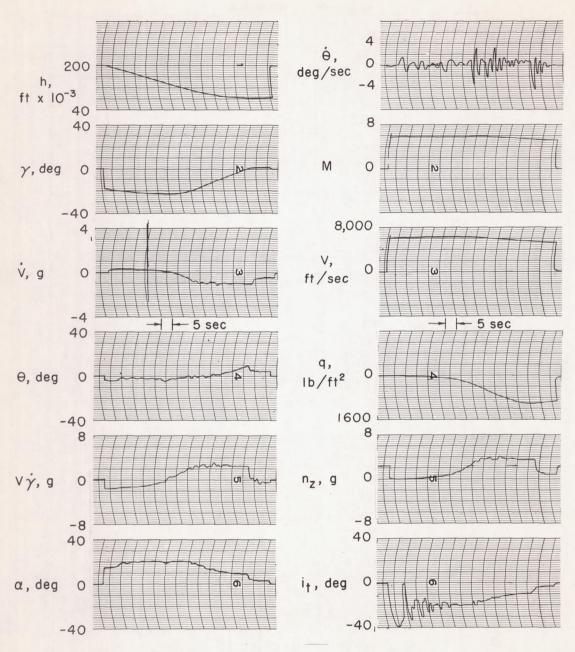
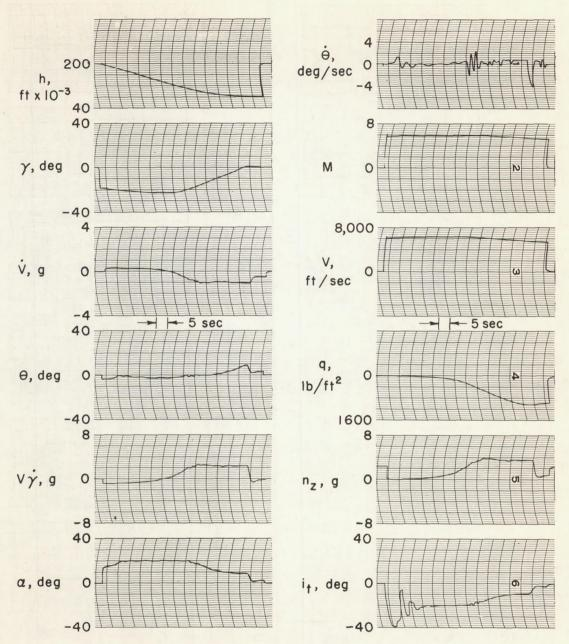


Figure 10.- Standard programmed entry flight; computed dynamic characteristics for four values of gearing of artificial-damping feedback.

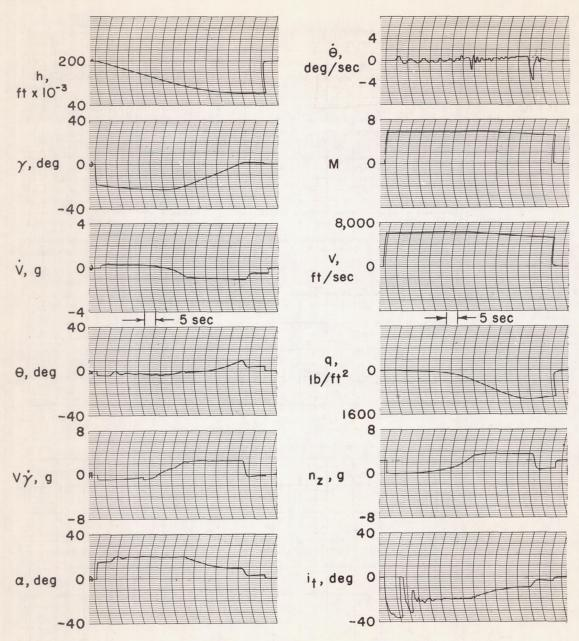


(a) Artificial-damping feedback gearing, $K_gK_s = -0.25$. Figure 11.- Standard piloted entry flight.



(b) Artificial-damping feedback gearing, $K_gK_S = -0.6$.

Figure 11. - Continued.



(c) Artificial-damping feedback gearing, KgKs = -1.0.

Figure 11. - Concluded.

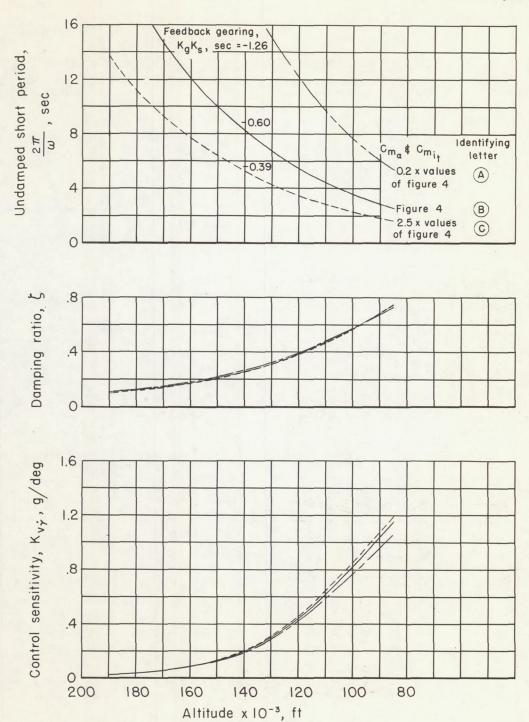


Figure 12.- Standard programmed entry flight; computed dynamic characteristics with $C_{m_{\alpha}}$, $C_{m_{\dot{1}\dot{1}}}$, and feedback gearings adjusted to give, predominantly, changes in period.

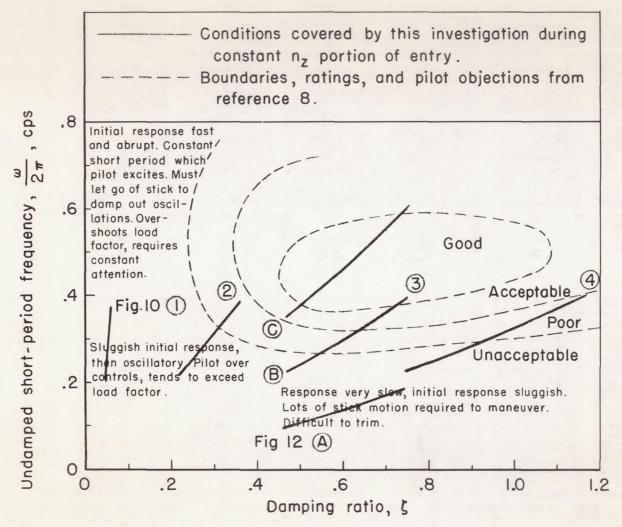


Figure 13.- Comparison of simulator results with those obtained in flight with a variable-stability airplane.

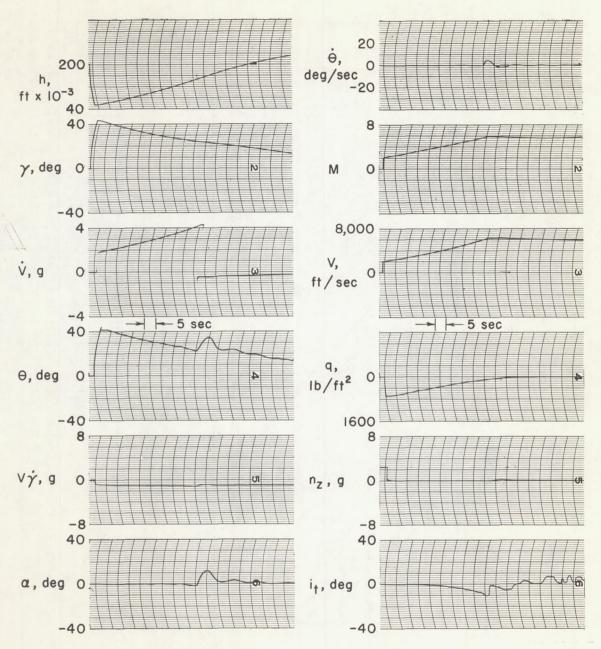


Figure 14.- A portion of a piloted ascent to 260,000-foot peak altitude, $K_gK_S = -0.6$.

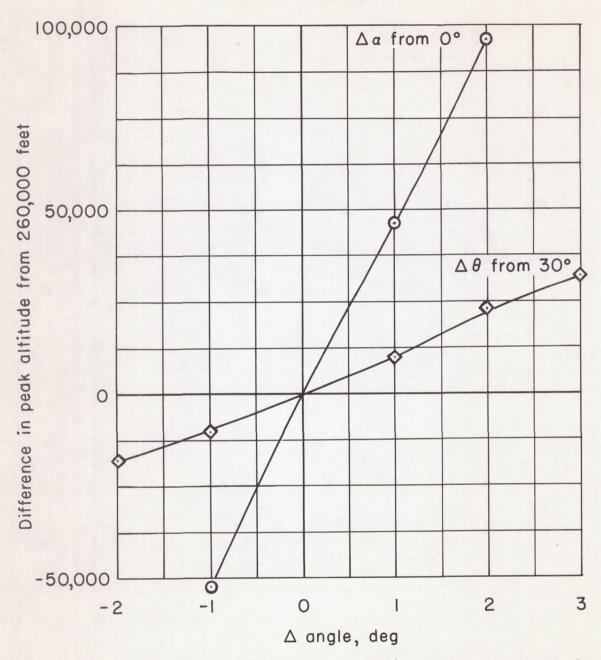


Figure 15.- Effect on peak altitude of a constant error in programmed angle during ascent.

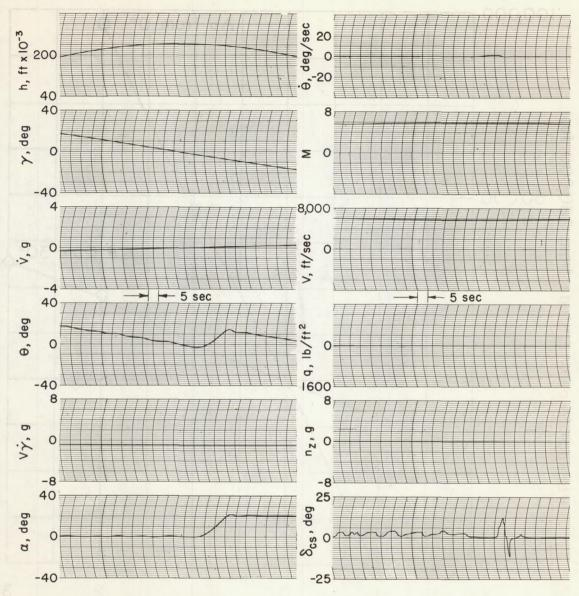


Figure 16.- Use of space control during ballistic portion of the trajectory.